

# The characteristics of direct current UV lamps and their effects on curable films

*Kiyoko Kawamura, Kazuo Ashikaga, & Teruo Orikasa*  
*Fusion UV Systems Japan KK*  
*Tokyo, Japan*

## 1. Introduction

It has been about 50 years since UV curable ink was first introduced to the printing industry – ink that ‘dries’ in an instant when irradiated with UV light. Up to now, the application of UV curable materials has been extended to a variety of fields beyond printing, and the materials have been developed as high functional materials offering high added value. The target goal of such materials is not only to “dry” materials, but also to provide high value-added products by UV irradiation. In particular, the importance of UV curing technology has been widely appreciated, since it is used for producing a variety of optical films for flat panel displays (FPDs) as well as optical recording media such as CDs and DVDs.

Not so much attention has been paid to light sources in application fields. However, the recognition about light sources is changing, since it is found in some application fields that the functional properties provided by UV curing reactions are strongly affected by UV emitting light sources. The UV curing process determines the final properties of UV curable materials, but the source that emits UV light is not merely a light-emitting device. The emission behavior of the light source also has a significant influence on the crosslinked microstructure, playing a crucial role in determinant of the final properties of cured materials.

The UV curing reaction is actually a 3-dimensional cross-linking reaction by photo-initiated polymerization, and the cross-linked networks are formed by propagation reactions starting at initiation points (radical generation points). According to Kloosterboer, et al.<sup>1-4</sup>, in the first stage of polymerization, microgels are generated at the polymerization initiation points, and with time these develop into macrogels. The macrogels are further combined in termination reaction, forming large cross-link networks. UV cured materials therefore have a microstructure that is inhomogeneous around the initiation points, and the microstructure can be changed considerably depending on the generation

state of initiation species. The inhomogeneity is the most significant characteristic of the cross-linked structures obtained by UV curing reaction, differentiating them from homogenous cross-linked structures produced by thermal curing reactions.

In this paper, UV curing reaction efficiency and the microstructure of cured films<sup>5</sup> induced by the differences in the light emission profile are examined. The effect of emission profile of light source on UV curing reaction mechanism is also examined from polymerization kinetics point of view.

## 2. Electrode lamp experiments

The alternating current is a familiar means for igniting electrode lamps, which utilize arc discharge from a filament. In order to investigate the effect of the lamp's supply current on emission profile, ignition tests were conducted on an electrode lamp connected to a fully rectified direct current supply. The emission profiles of the lamp ignited by AC and also DC power supplies were measured by passing a radiometer (EIT UV Power Map, sampling with 2048Hz) beneath the lamp. The same lamp was used in both experiments. Figure 1 shows the emission profile obtained by each power supply and an expanded view of the time axis<sup>6</sup>. It is clear from the profiles that the DC lamp emits light smoothly over time with no sharp fluctuations in intensity. Such light emission is known as 'steady state light'. In contrast, the emission profile of conventional electrode lamp shows waves or ripples over time, resembling a pulsated emission. Their emission intervals are about 8.3 milliseconds and correspond to the alternating current cycle (emission using 60Hz supply).

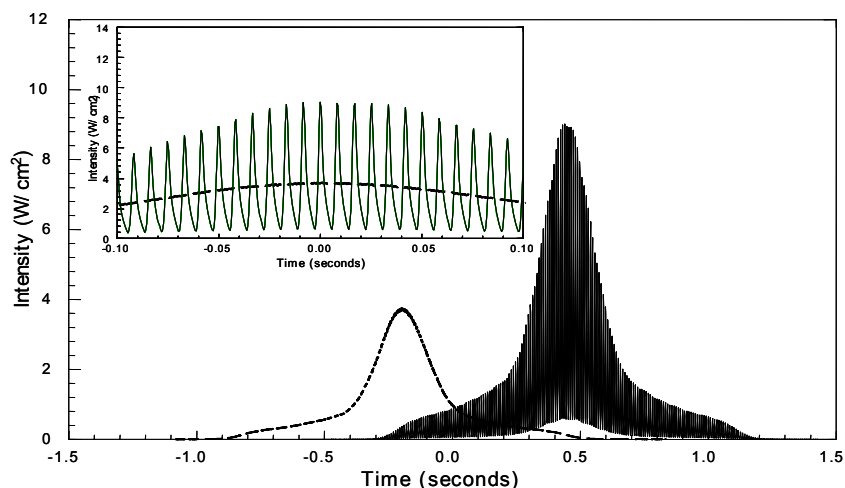


Figure 1 Emission profiles obtained from an electrode lamp ignited by alternating current (—) and direct current (---)

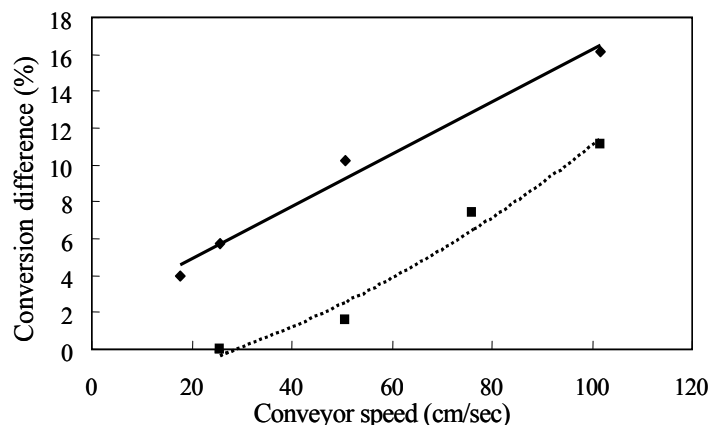


Figure 3 Conversion differential between irradiation under DC and AC electrode lamps ( —◆— in N<sub>2</sub>; .....■ in Air). The conversion differential increases with decreasing irradiation energy. The conversion differential is large in N<sub>2</sub> in which radicals have longer lifetime.

In order to examine the effect of light emission profiles on UV curing reactions, photo-initiated polymerization of isobornyl acrylate was examined by using both lamp systems. 1-Hydroxy-cyclohexyl-phenyl-ketone (Ciba IRGACURE184) was used as an initiator in the polymerization system. The conversion yield for polymerization was obtained by measuring the amount of residual double bonds of isobornyl acrylate by means of FTIR. Figure 2 shows the conversion obtained by irradiation in both nitrogen and air environment<sup>5</sup> against conveyor speed.

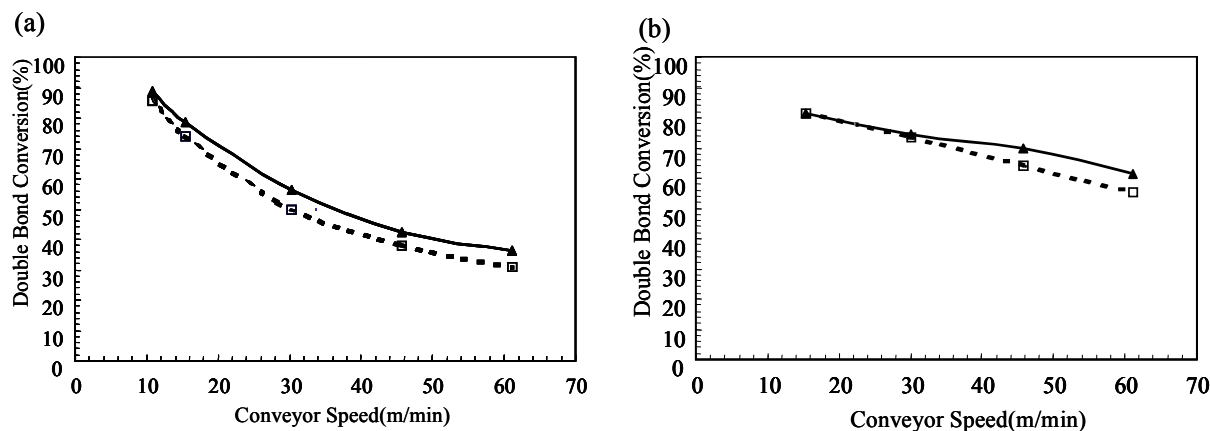


Figure 2 Photo-initiated polymerization conversion of isobornyl acrylate, (a) Conversion in N<sub>2</sub> with 0.25% IRGACURE 184, (b) Conversion in air with 2% IRGACURE 184, .....□..... : Irradiation by AC ignited electrode lamp, —▲— : Irradiation by DC ignited electrode lamp

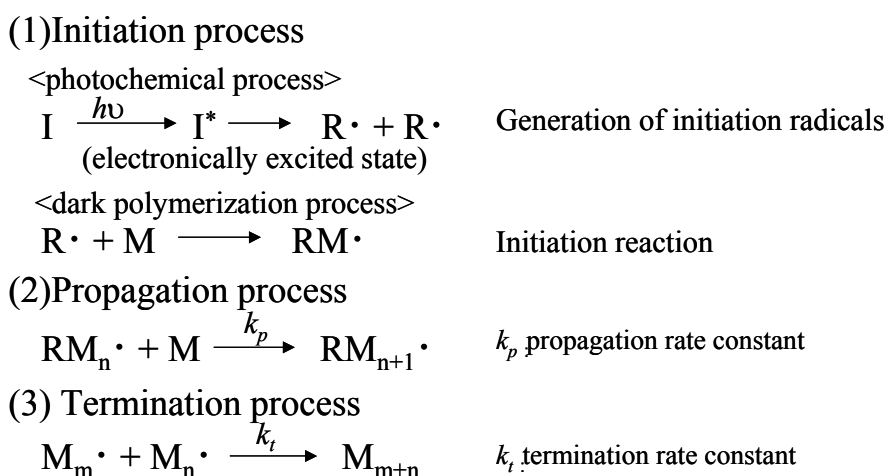
It is shown in Fig. 2 that the irradiation by the DC light source provides higher conversions than by the AC under all irradiation conditions. The differential between the conversions obtained by the DC light irradiation and the AC was plotted against the conveyor speed, as shown in Fig.3. As can be seen in

the figure, the conversion differential increases with increasing conveyor speed (decreasing irradiation energy). It is also shown that this conversion differential is expanded in the nitrogen gas environment, in which the radicals have longer lifetime.

These results indicate that the emission profile of the UV irradiation light greatly affects on the reaction conversions.

### 3. Factors contributing to conversion differential

The influence of emission profiles on the reaction conversion is discussed in this section. As mentioned before, the UV curing reaction creates a 3-dimensional cross-link by photo-initiated polymerization. Each process of the polymerization is shown in Scheme 1.



Scheme 1. Photo-initiated polymerization scheme

As shown in the scheme 1, UV light is engaged only in the primary stage of initiation reaction, in order to form electronically excited states of initiator molecules. The excited singlet or triplet states of initiator molecules is formed by the UV light absorption, and the molecules in the excited states give rise to intramolecular cleavage or hydrogen abstraction reactions. The initiation radicals, electronically ground state, for polymerization are generated via these reactions. A lifetime of molecules in each excited state is generally in the order of nanoseconds for excited singlet state and microseconds for the excited triplet state at room temperature. As described above, the emission intervals in ripple irradiation are in the order of msec. Therefore, taking a lifetime of the electronically excited species into account, the time period with no light emission is long enough and no reactive species are generated in the dark time period during irradiation. In other words, the time period in which only propagation and termination reactions occur exists under ripple irradiation. The steady state in which the initiation rate is equal to the termination rate is not established in ripple irradiation from the reaction kinetics point of view.

Based on the above scheme 1, the polymerization propagation rate,  $R_p$ , is given by Eq.1, as follows.

$$R_p = (k_p/k_t^{1/2})(\phi I_a/2)^{1/2} [M] \quad (\text{Equation 1}).$$

In Eq. 1,  $k_p$  is the propagation rate constant and  $k_t$  is the termination rate constant,  $\phi$  is the quantum yield of radical generation of initiator molecule,  $I_a$  is the quanta of light absorbed by the initiator, and  $[M]$  is the concentration of monomer (concentration of double bonds). In the photo-initiated polymerization of isobornyl acrylate described above, the  $(\phi I_a/2)^{1/2} [M]$  term of Eq. 1 is the same for both steady state light and ripple-light irradiations. Therefore the conversion difference is caused by the values for  $(k_p/k_t^{1/2})$ . However, the  $k_p$  value is the same because of using same isobornyl acrylate in both systems. The conversion differences between two different light sources must be attributed to the different  $k_t$  values. The  $k_t$  values have about  $10^6 \sim 10^8 \text{ M}^{-1}\text{s}^{-1}$  order and the  $k_p$  values have  $10^3 \sim 10^5 \text{ M}^{-1}\text{s}^{-1}$  order,  $k_t$  values has  $10^3 \sim 10^4$  times of  $k_p$  and affect on polymerization rate. It is considered that the observed termination rate is faster under the ripple irradiation like pulse than under the steady state light produced by direct current.

The recombination of radicals between two propagating polymers (“normal” termination) is the major termination process under the steady state light irradiation. However, under the ripple irradiation, the proportion of the different termination reaction other than ‘normal’ termination increases in the termination process of propagation radicals, since only propagation radicals (no initiation radicals) as the reactive species exist at the dark time period in the polymerization. In such a polymerization process, a low molecular weight radical (e.g. initiator radical) generated by the subsequent pulse-like irradiation rapidly attacks a propagation radical produced by the former pulse-like irradiations. In other words, the low molecular weight radicals, having higher mobility than propagation radicals, continually generated by intermittent irradiation give rise to “premature” termination for the terminal propagation radicals of polymer chain<sup>7,8</sup>. As the result, the ripple irradiation system shows a higher  $k_t$  and lower  $R_p$  value than the DC irradiation system, and the difference in  $R_p$  values provides the conversion differences between the irradiation systems. A schematic representation of the two different types of termination reaction is shown in Fig. 4.

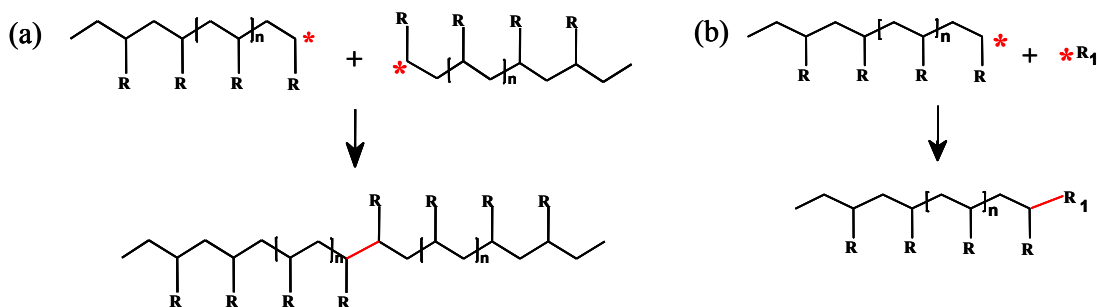


Figure 4 Schematic representation of termination process by radical recombination, (a) “Normal” termination by recombination by propagation radicals, (b) “Premature” termination by low molecular weight radicals generated by intermittent UV irradiation.

#### 4. Emission profiles of electrode-less lamps and photo-initiated polymerization

The microwave lamps are electrode-less and emit light with microwave energy generated by magnetron. The magnetron works with the direct current, however, there are two systems to obtain electric current. One is full-wave rectified alternative current shown in Fig. 5 (a) and the other is completely direct current in Fig. 5 (b). The emission profile of the lamp system worked by the full-wave rectification current shows ripple emission which is similar to that obtained by electrode lamps, due to the influence of waveform of electric current. In contrast, DC lamp system shows continuous emission (steady state light). The interval of ripple emission in Fig. 5 is 10ms under the 50Hz-rectified current. The

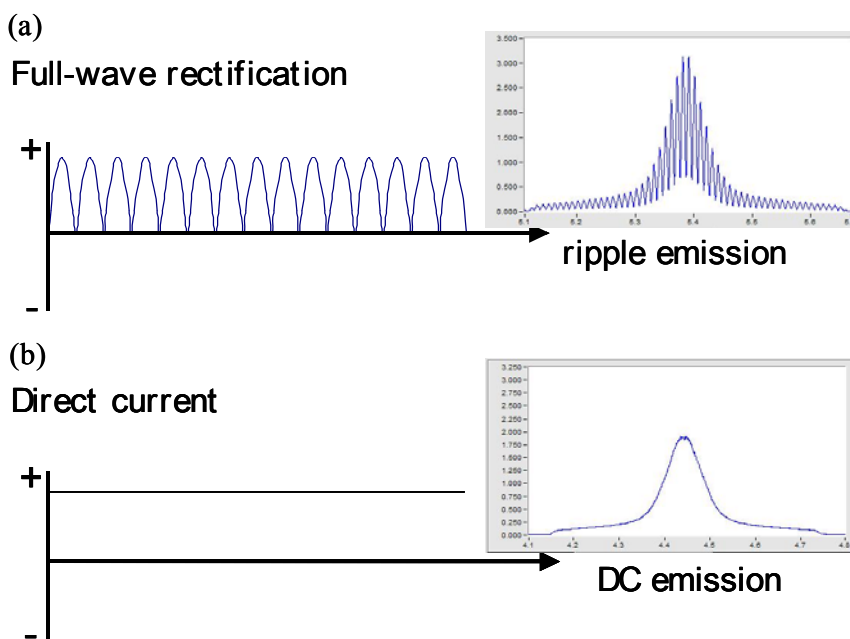


Figure 5 Emission profiles of the lamp systems, (a) emission with the 50Hz rectified current, (b) emission with direct current.

photo-initiated polymerization has been done, by irradiation with two lamp systems, in order to obtain fundamental information about UV curing reaction.

In the actual UV curing systems, it is almost impossible to analyze polymerization behavior, since the polymerized materials are insoluble, due to the 3 dimensional cross-link structure. In order to examine the effect of the differences between two lamp systems on photo-initiated polymerization, the mono-functional monomer was used in a series of the experiments. The obtained polymers were analyzed by GPC.

Benzyl acrylate was used as a mono-functional monomer and 1 wt% Irgacure184 was added in the monomer as a photo-initiator. The UV irradiation was carried out under the nitrogen environment (oxygen concentration: ca. 500ppm).

The obtained results are shown in Fig. 6. Figure 6(a) shows the molecular weight distribution (Mw/Mn) of benzyl acrylate polymer. As can be seen in the figure, the polymers obtained by the DC irradiation show smaller Mw/Mn values (narrower molecular weight distribution), than those obtained by the ripple irradiation in all irradiation energies. In addition, the differences of Mw/Mn values between two irradiation systems tend to expand in higher irradiation energy region. That is, the DC irradiation system gives almost constant Mw/Mn values against all irradiation energies, on the other hand, the Mw/Mn value of the ripple irradiation system increases with increasing irradiation energy.

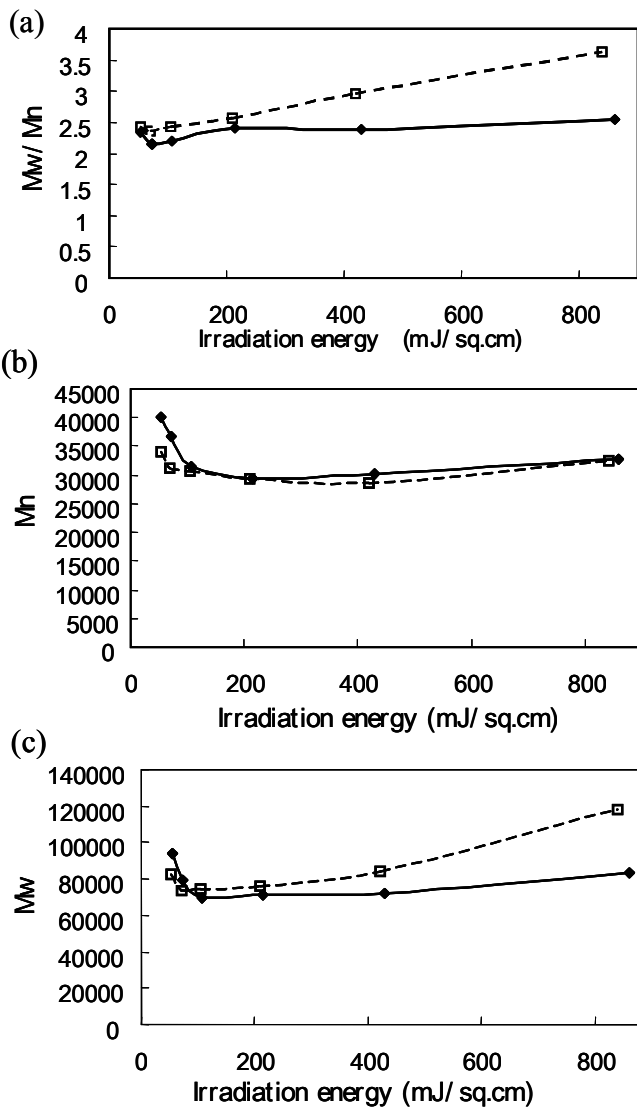


Figure 6 GPC measurements of benzyl acrylate against irradiation energy. (a) the molecular weight distribution,  $M_w/M_n$ , (b) the number average molecular weight,  $M_n$ , (c) the weight average molecular weight,  $M_w$ ; —◆— DC irradiation, .....□..... ripple irradiation

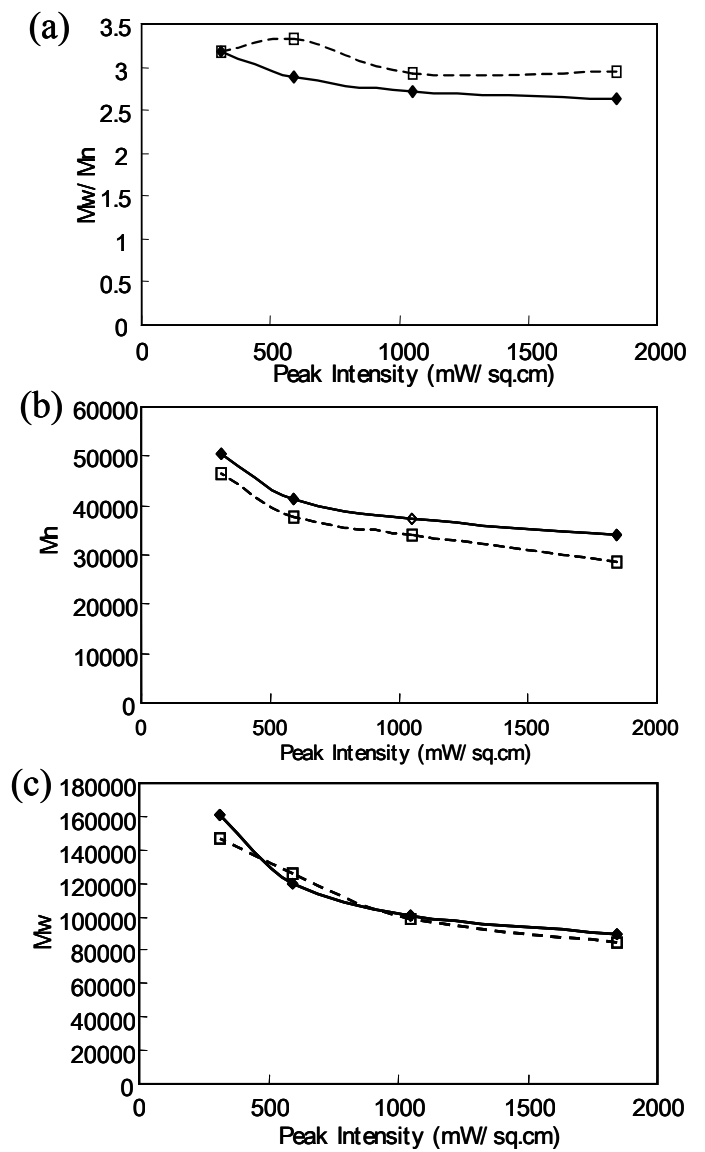


Figure 7 GPC measurements against the irradiation intensity. (a) the molecular weight distribution,  $M_w/M_n$ , (b) the number average molecular weight,  $M_n$ , (c) the weight average molecular weight,  $M_w$ ; —◆— DC irradiation, .....□..... , ripple irradiation

The number average molecular weight ( $M_n$ ) for the obtained polymers also depends on the emission profiles, especially lower irradiation energy less than  $100 \text{ mJ/cm}^2$ , as shown in Fig. 5(b). The polymers obtained by the DC emission irradiation show high  $M_n$  values, compared to the polymers obtained by the ripple emission irradiation. On the other hand, the weight average molecular weight ( $M_w$ ) shows different tendency for these polymers. The  $M_w$  value of the polymer obtained by the ripple emission irradiation increases with increasing irradiation energy and is higher than that obtained by the DC irradiation. The DC irradiation provides almost constant  $M_w$  value for the polymers in all irradiation energies.

The irradiation intensity dependence for molecular weight with two photo-irradiation systems was also examined. The obtained results were summarized in Fig. 6. The total irradiation energy was adjusted to be  $420 \text{ mJ/cm}^2$  in each irradiation. Figure 7(a) shows the  $M_w/M_n$  values for each irradiation system. As shown in the figure, the  $M_w/M_n$  values obtained by the DC emission irradiation are smaller than those obtained by the ripple irradiation in all irradiation conditions. Since the DC irradiation brings higher  $M_n$  values, compared to the ripple irradiation, the  $M_w/M_n$  values obtained by the DC irradiation show smaller values than those obtained by the ripple irradiation, although the  $M_w$  values obtained by both irradiations are almost same.

It is considered that the differences of molecular weight between two irradiation systems reflect the difference of premature termination efficiency of propagation radicals during polymerization. The number of radicals generated by the same irradiation energy is same between two irradiation systems. That is, the amount of polymer molecules generated is essentially same in each irradiation system, and the molecular weight of polymer is controlled by effective concentration of propagation radicals and their lifetime. In the photo-initiated polymerization of benzyl acrylate, the lifetime of propagating radical is unknown under 500ppm oxygen concentration at this moment. However, the effective concentration of propagation radicals can be compared relatively between two irradiation systems. In low irradiation energy condition, the effective concentration of propagation radicals in the ripple irradiation system is lower than the DC irradiation system, because the premature termination of propagation radicals by the newly generated radicals from initiators takes place more efficiently in the ripple irradiation system. In high energy irradiation condition, the termination mechanism is essentially same as low irradiation condition in early stage. However, due to high number of photon irradiation, the effective concentration of the propagation radicals is much higher, compared to low energy irradiation condition. As the result, high molecular weight polymer fraction is increased by the ripple irradiation with high energy irradiation.

Under the same irradiation energy shown in Fig. 7, the molecular weight of the obtained polymer depends on the irradiation intensity, that is, the molecular weight decreases with increasing irradiation intensity, which is general tendency for radical polymerization. As for the  $M_n$  values, the polymers obtained by the DC irradiation show apparently higher  $M_n$  values than those obtained by the ripple irradiation. It is suggested that the effective concentration of propagation radicals generated by the DC irradiation is higher than that generated by the ripple irradiation, due to less premature termination of propagation radicals in the DC irradiation systems.

As described previously, the UV curing reaction brings about the formation of an inhomogeneous crosslinked structure, and it is presumed that a greater number of micro/macro gels are formed under the ripple irradiation at the initial stage, compared to the DC irradiation, since the premature termination takes place more frequently under the ripple irradiation. In order to visually examine microstructure of cross-linked materials, the trimethylol propane triacrylate (TMPTA) film at an early stage of curing was observed by a phase contrast microscope. Because the double bonds of acrylic group in TMPTA are converted into the single bonds by UV irradiation, the refractive index of TMPTA is changed after irradiation. It is possible, especially in early stage of curing reaction, to directly observe the refractive index differential of cured domains by using the phase contrast microscope.

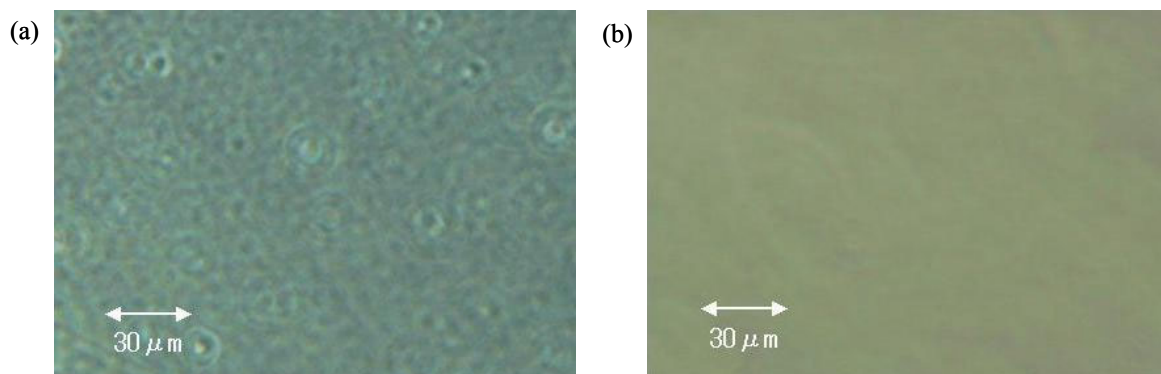


Figure 8 Phase contrast micrograms of cured film of TMPTA with 1% Irgacure 184 (optically inhomogeneous curing domains are visible, formed by ripple irradiation) (a) obtained by ripple irradiation, (b) obtained by DC irradiation

Figure 8 shows phase contrast micrograms of the cured TMPTA films (thickness: approximately 100  $\mu\text{m}$ ) irradiated with a full-wave rectification electrodeless lamp and a DC electrodeless lamp. The cured film obtained by ripple irradiation shows micro-domain formation. In contrast, such kind of micro-domain structure was not observed for the film cured with the DC irradiation. It is suggested

that the observable micro-domains by optical microscopy are not formed with irradiation by the DC lamp. The premature termination reaction occurs more readily under ripple irradiation, and it induces micro-domain structure shown in Fig. 8.

## 5. Conclusion

The cross-linked structure provided by UV curing reaction is by nature inhomogeneous, however, the irradiation light source has a considerable influence on the curing conversion and the micro-domain structure of cured material. Not so much attention has been paid to the emission profiles and characteristics of irradiation light sources in the UV curing process. But growing the application fields of UV curing technology, the technology is used to produce high performance materials. The nature of emitting light from light sources is one of the important key technologies in such application areas, because such high properties, in most cases, are closely linked to the microstructure of the cured material. It is now possible to achieve the steady state light irradiation by using UV irradiation devices powered by direct current, which reduces the “premature” termination process in UV curing reactions. It is likely that UV curing technology will continue to be used for developing new high performance materials in a lot of fields, and the DC lamp is expected to make a large contribution in such application fields, as the UV irradiation light source.

## 6. References

- 1) J.G. Kloosterboer: Adv. Polym. Sci., 84, 1 (1988)
- 2) J.G. Kloosterboer: Adv. Polym. Sci., 84, 8 (1988)
- 3) J.G. Kloosterboer, B.M.M. Hei, & H.M. Boots: J. Polym. Commun., 25, 354 (1984)
- 4) H.M. Boots, J.G. Kloosterboer, & B.M.M. Hei: Br. Polym. J., 17, 219 (1985)
- 5) Ashikaga, Kazuo & Kawamura, Kiyoko: Industrial Coating [*kougyou tosou*], 201, 40 (2007)
- 6) S. Jonsson, et al.: 14<sup>th</sup> Fusion UV Technology Seminar Proceedings, p. 14.
- 7) J.E. Elliott & C.N. Bowman: Macromolecules, 32, 8621 (1999)
- 8) J.E. Elliott & C.N. Bowman: Macromolecules, 34, 4642 (2001)